

Air/Sea Interaction in the Western Tropical Pacific Ocean during 1982/83 and 1986/87

Gary MEYERS, Rick BAILEY, Eric LINDSTROM and Helen PHILLIPS

*CSIRO Division of Oceanography
GPO Box 1538, Hobart Tasmania 7001, Australia*

ABSTRACT

The Southern Oscillation Index (SOI), equatorial zonal wind, sea level anomalies at islands, sea surface temperature at Puerto Chicama Peru and mixed layer temperature and depth from the XBT ship-of-opportunity network are used to describe conditions during the past two ENSO episodes. Onset of sustained ENSO anomalies in the 1986/87 episode was in July 1986, one month later in the year than onset of the 1982/83 episode in June 1982. Both episodes of the 1980's developed later in the year than episodes of the 1970's. The XBT data show that during the episodes of the 1980's the usual surface temperature difference along the equator between 165°W and 160°E reversed and rapidly increased to 1°C in the other direction. ENSO warming of the central Pacific tends to be confined to the region 10°N-10°S whereas cooling of the western Pacific occurs in a broader region from 19°N-19°S, and extends westward into the eastern Indian Ocean. Evaluation of terms in the surface heat budget (for 1982/83 episode only) shows that the dominant mechanism of cooling surface temperature in the western Pacific is latent heat flux.

1. Introduction

The largest pool of warm (>28°C) surface water in the global ocean is located in the western Pacific and eastern Indian Oceans. The overlying air is also warm, giving it the capacity to hold a very large load of water vapour, relative to other tropical, marine air masses. Release of latent heat by deep atmospheric convection over the heat pool provides one of the main sources of energy for the global atmospheric circulation (Hénin and Donguy, 1980; Donguy, 1987). Air/sea interaction in this area has since the 1920's been recognised as an important factor in El Nino/Southern Oscillation (ENSO) (Berlage, 1966; Nicholls, 1989). The basic observation was an association between anomalous cooling in the area and the occurrence of drought, especially in Australia. It was suggested that, theoretically at least, cooling during ENSO could be caused by ocean currents, mixing of cool water from the thermocline into the surface layer, of heat fluxes at the sea surface; the dominant cause was not identified. A surface heat budget near the equator, at 160°E (Meyers et al., 1986) indicated that latent heat flux was an important factor in the cooling. In part the goal of this study is to expand earlier study into a wider area, drawing on results from Meyers et al. (1989a), and to extend the study in time to describe the 1986/87 ENSO episode.

The mature stage of this episode occurred in mid 1987 (Halpern, 1988) and it was characterized using definitions by Quinn et al. (1987) as weak-moderate in intensity (Quinn, personal communication, 1989). An aim of this study is to describe air/sea interaction associated with onset of the episode.

2. Data

Four standard indices of ENSO - a Southern Oscillation Index (Fig. 1), equatorial zonal wind (Fig. 2), Pacific sea level anomalies west of the dateline (Fig. 3) and sea surface temperature at Puerto Chicama, Peru (Fig. 4) - were assembled to determine the time of onset



F 30211

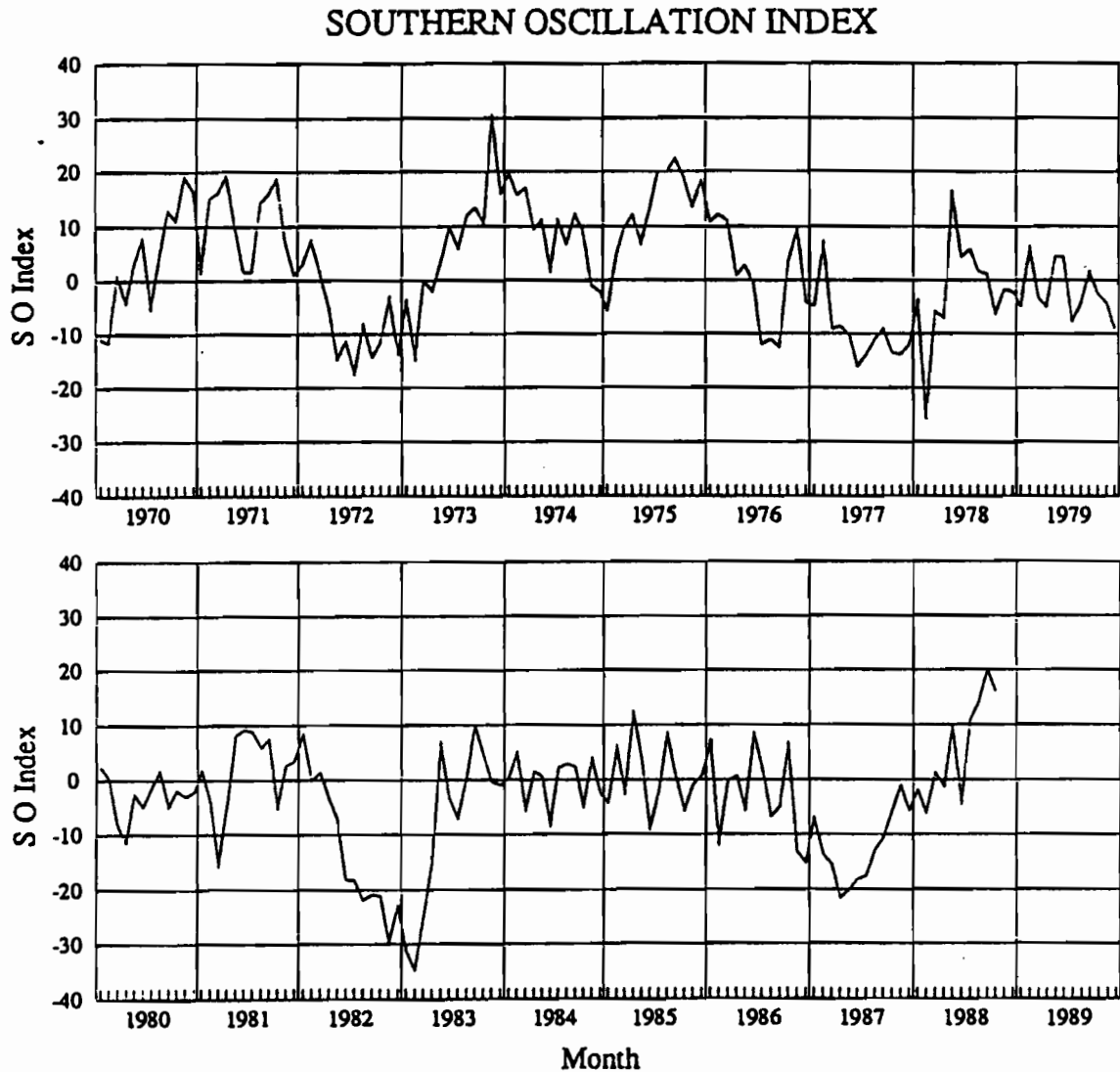
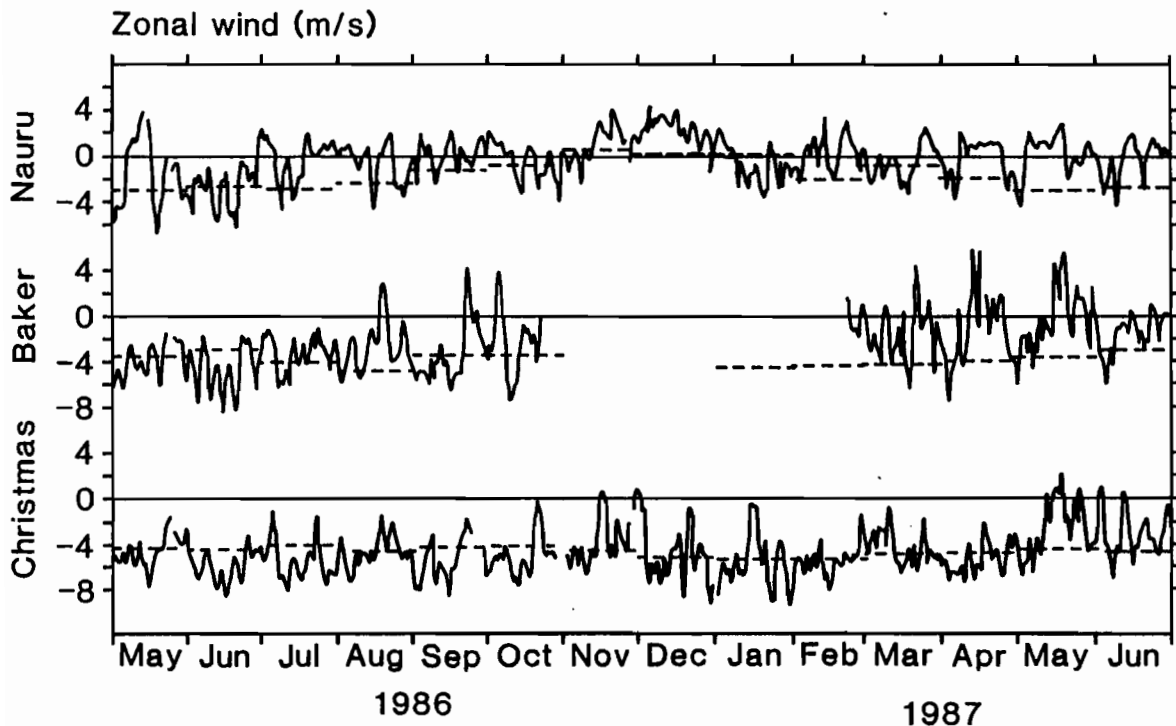


FIG.1. Southern Oscillation Index

for the last two episodes and to compare them to earlier episodes in the 1970's. The Southern Oscillation Index (SOI) is determined from barometric pressure at Tahiti and Darwin, seasonally adjusted with a 100 year record, and normalized to a standard deviation of 10. It is a very long time series, available since 1882, and the update is published monthly by the regional Bureau of Meteorology in the Darwin Tropical Diagnostic Statement (Halpern, 1988). The relationship of this index to the global field of barometric pressure has been discussed by Trenberth and Shea (1987). The sea level anomalies west of the dateline were averaged at 10-15 stations in the latitude band 15°N - 15°S . The climatological monthly mean sea level used to evaluate anomalies was for the period 1975-1981. Maps of the anomaly are distributed monthly by K. Wyrski and G. Mitchum of the University of Hawaii (Wyrski et al., 1988). Sea surface temperature at Puerto Chicama was made available by electronic mail in near real time by D. Enfield of NOAA/AOML, in the form of monthly averages. It was compared to two climatologies for the periods 1925-1973 (A. Douglass, personal communication) and 1956-1982 (D. Enfield, personal communication). The use of Puerto Chicama SST as an index of El Niño and its relationship to the Southern oscillation has been



P. Freitag (Clim. Diag. Bull.)

FIG.2. Equatorial zonal wind ($\text{m}\cdot\text{s}^{-1}$) at Nauru, Baker and Christmas Islands.

discussed by Deser and Wallace (1987). The equatorial zonal wind index is based on daily values from island stations (McPhaden et al., 1988). The climatological values of Wyrtki and Meyers (1976) for the period 1900-1972 were used for comparison to normal monthly conditions. The wind indices were distributed in the US Climate Analysis Center's Climate Diagnostic Bulletin (Halpern, 1988).

Data from the TOGA expendable bathythermograph (XBT) ship-of-opportunity network (Donguy, 1987; Meyers et al., 1989a, b) were used to measure ocean thermal structure of the tropical Pacific and eastern Indian Oceans. The data permit a description of mixed layer temperature and depth and, using additional data on surface heat fluxes from Reed (1986), the dominant terms in the mixed layer heat budget are assessed.

3. Onset of the 1986/87 episode

Understanding the onset of ENSO is one way to improve models for its prediction. Past studies have suggested two scenarios of onset (see Lukas and Webster, 1988 for a review), depending on where the fundamental precursor is found, either in the ocean or the atmosphere. In one scenario, propagating oceanic signals carrying the seed of an ENSO episode are present throughout an entire ENSO cycle, and at a certain stage they amplify through an instability. The onset in this case might be associated with the oceanic signals just before they amplify. In the second scenario anomalous equatorial, westerly winds (possibly related to tropical-extra tropical atmospheric interaction) trigger an instability of the coupled ocean and atmosphere, which intensifies into a mature episode. The onset in this case would be determined by the time when sustained ENSO-type anomalies in the atmosphere first develop. The two scenarios are not necessarily mutually exclusive (Lukas, 1988) if the propagat-

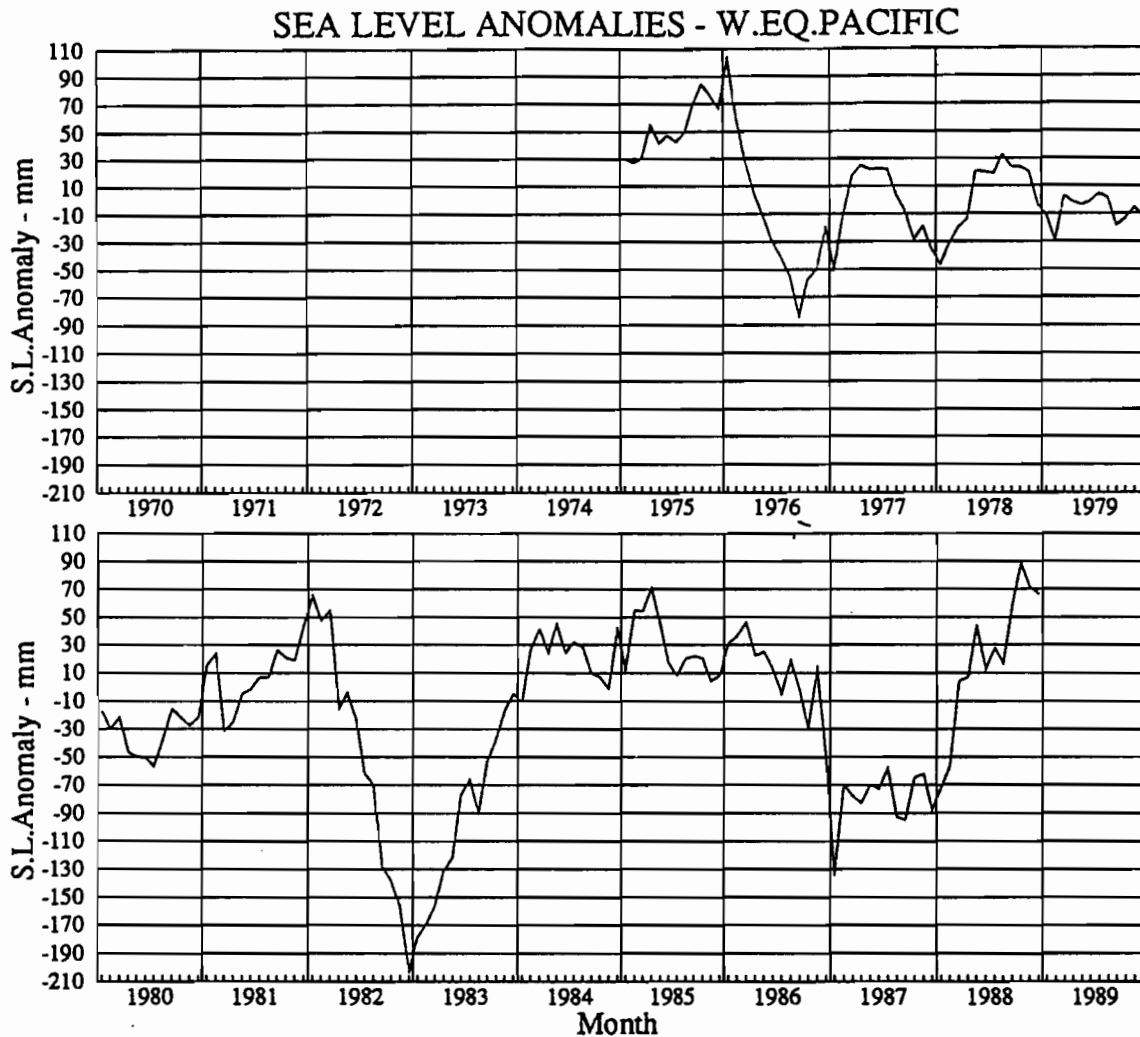


FIG.3. Average sea level anomaly (mm) western Pacific, 15°N-15°S, west of the dateline.

ing oceanic signals affect SST patterns, and through air-sea interaction, the wind field. We have looked for the 1986/87 onset in atmospheric parameter (Figs.1 and 2) and for the growing instability in oceanic parameters (Figs. 3 and 4). Whether or not the prediction issued in 1986 (Cane et al., 1986) successfully predicted the episode for the right reasons - that is, predicted it because the real episode in nature evolved with largely the same dynamics as in the model - can be partly decided in future studies by comparing models to the observed parameters.

Beginning with the SOI (Fig. 1) and equatorial zonal wind at Nauru (Fig.2) we see the onset of sustained ENSO-type anomalies in July 1986. A brief hiatus in October in both indices is followed by steady development to mature ENSO anomalies in March-June 1987 (Halpern, 1988), particularly evident in the zonal wind at Baker and Christmas Island. Changes in the wind field will produce dynamically consistent changes in the ocean. The development of the equatorial wind anomaly changes the structure of the field of trade winds in the western Pacific in a way that makes wind stress curl favourable for upward Ekman pumping of the thermocline (Pazan and Meyers, 1982; Donguy et al., 1982; Harrison et al., 1989). The rise in thermocline, and depletion of warm water in the upper layer should lead to a drop in sea level.

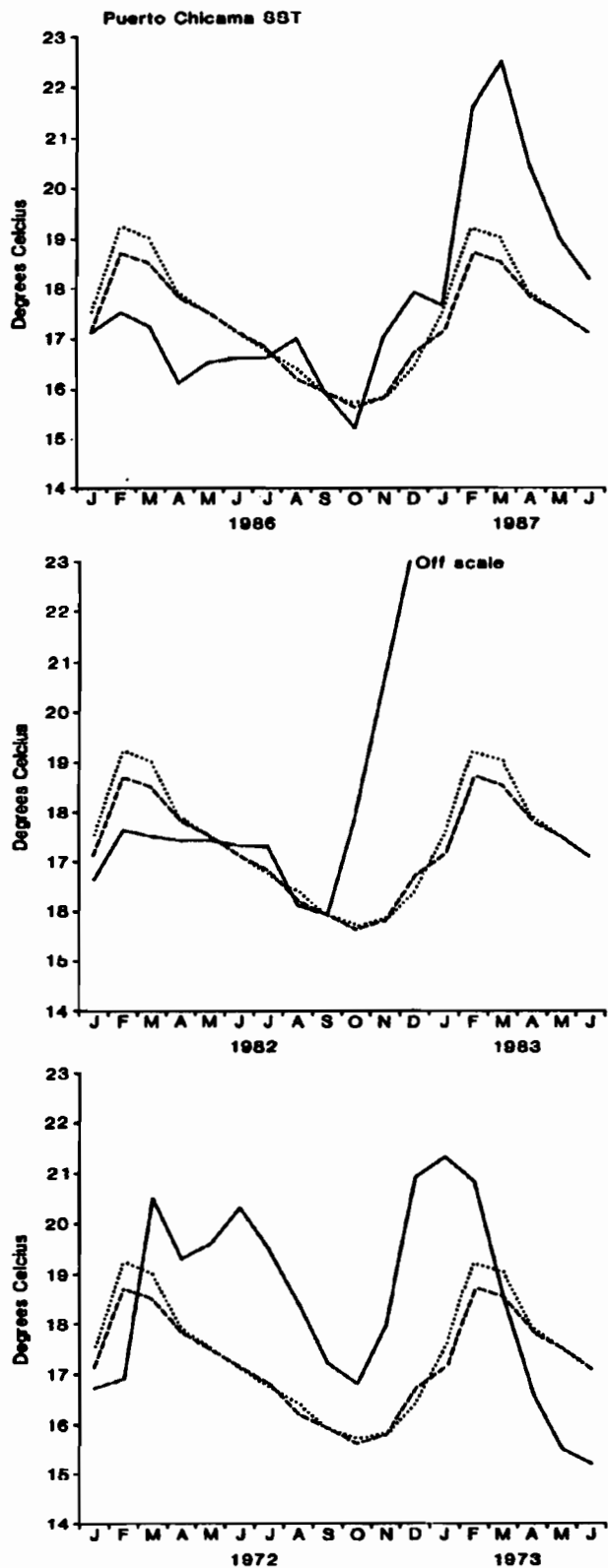


FIG.4. Sea surface temperature at Puerto Chicama, Peru during the ENSO episodes of 1986/87 (top), 1982/83 (middle) and 1972/73 (bottom), compared to the mean annual cycle, 1925-1973 (dotted line) and 1956-1982 (dashed line).

The westerly wind is also expected to generate anomalous eastward currents and downwelling which propagate to the eastern Pacific as Kelvin waves and affect the surface heat budget there (Harrison et al., 1989).

The sea level of the western Pacific (Fig. 3) and temperature at Puerto Chicama (Fig. 4) show the corresponding development of anomalies. Sea level near the area of westerly wind developed sustained ENSO anomalies after August 1986, and except for a hiatus in November, rapidly reached levels of 7-11 cm below normal which were maintained throughout 1987. SST at Puerto Chicama rapidly increased after October 1986, reaching a peak in March 1987 with an anomaly in excess of 3°C, and it remained above normal at least until June 1987.

The atmospheric changes (Fig's 1 and 2) and expected response on either side of the ocean indicate in a dynamically consistent way that the onset of sustained ENSO type anomalies was in July 1987 (McPhaden et al., 1988).

Earlier in the year, bursts of equatorial, westerly wind were recorded near the dateline in January and May 1986 (McPhaden et al., 1988; Lander and Morrissey, 1988). The event in May generated an expected local response in the ocean; and a remote response carried by a Kelvin wavelike pulse (McPhaden et al., 1988), which arrived at 0°, 110°W in late June. The development of a slightly positive SST anomaly at Puerto Chicama (Fig. 4) and increasing temperature at other stations on the Peru Coast in late July (D. Enfield, F. Chavez, personal communications, 1986) may signal the passage of the Kelvin wave. The anomaly, however, did not persist, and normal seasonal cooling resumed at Puerto Chicama after August. Our indices (Fig's 1-4) agree with the conclusion of McPhaden et al., that the burst in May did not generate sustained ENSO type anomalies and the feedback between ocean and atmosphere necessary to generate ENSO did not occur. The onset is discussed further in analyzing temperature along the equator on TOGA XBT tracks.

4. Comparison to earlier episodes

The four ENSO episodes which have occurred since 1970 (1972/73, 1976/77, 1982/83, 1986/87) were observed in each case with a quantum improvement in our capacity to document the ocean's dynamical role. In the case of 1972/73, the improvement was in understanding of the dynamics actually occurring in the ocean (Wyrski, 1975). By 1976/77 the number of sea level stations had increased to the extent that sea level maps could be drawn on an oceanic scale (Wyrski, 1985). By 1982/83 some of the outstanding improvements were an extensive network of XBT ships of opportunity to observe thermal structure to a depth of 400 m (Donguy, 1987), and longterm moorings established at a few sites along the equator for direct measurement of currents, (Halpern, 1987). The most important difference between 1986/87 and all the others was the relatively enormous resources to observe the ocean made available by the decade long (1985-1995) Tropical Ocean Global Atmosphere program (Halpern, 1988, for example) using in situ methods and remote sensing from satellites. Interpreting this great wealth of information will be one of the important activities of this conference. As a background to this task, we compare the 1986/87 episode to the earlier ones using the indices of Fig's 1, 3 and 4.

The SOI changes its nature somewhat over long time periods (Berlage, 1966) and the last two decades is not an exception. Before 1976 (Fig. 1) and extending back in time until 1950 (not presented) the SOI rose to levels above 10 for extended periods of several months. After 1976 the peaks did not develop for 12 years until 1988/89. Thus the 1986/87 episode was not preceded by the build-up of SOI associated with episodes of the 1950's, 60's and 70's, which are sometimes thought of as a canonical-type of ENSO (Rasmusson and Carpenter, 1982). The time of onset also changed for episodes after 1976, as seen most clearly in Puerto Chicama temperature (Fig. 4). The warming event at this station began in 1972 with a faster than normal rise in temperature during January/February, in the middle of the

season of normal summer heating. It began in 1982 in September, just before the normal cooling season ended and in 1986 it began about one month later, early in the warming season. In assessing the importance and generality of the great wealth of observations on the most recent episode, we should keep in mind the differences between ENSO episodes.

5. Mixed layer temperature and depth

The distribution of SST along the equator in the Pacific and Indian oceans is one of the most important factors in variability of the Global climate system because it influences the release of latent heat (ie. formation of rainfall) in the tropical marine atmosphere, and thus affects the supply of energy to global general circulation. Using the SST pattern for climate prediction requires an accurate descriptive knowledge of the evolution of SST, as well as an understanding of the processes that control the changing SST pattern (Meyers et al., 1989a; England et al., 1989). The interactive mechanism of SST gradients and surface wind convergence may be a major influence on deep convection in the tropical atmosphere (see Halpern, 1988 for a summary of relevant studies), but large scale temperature measurements before the 1980's were not accurate enough to record the small changes in the gradients of the central and western Pacific.

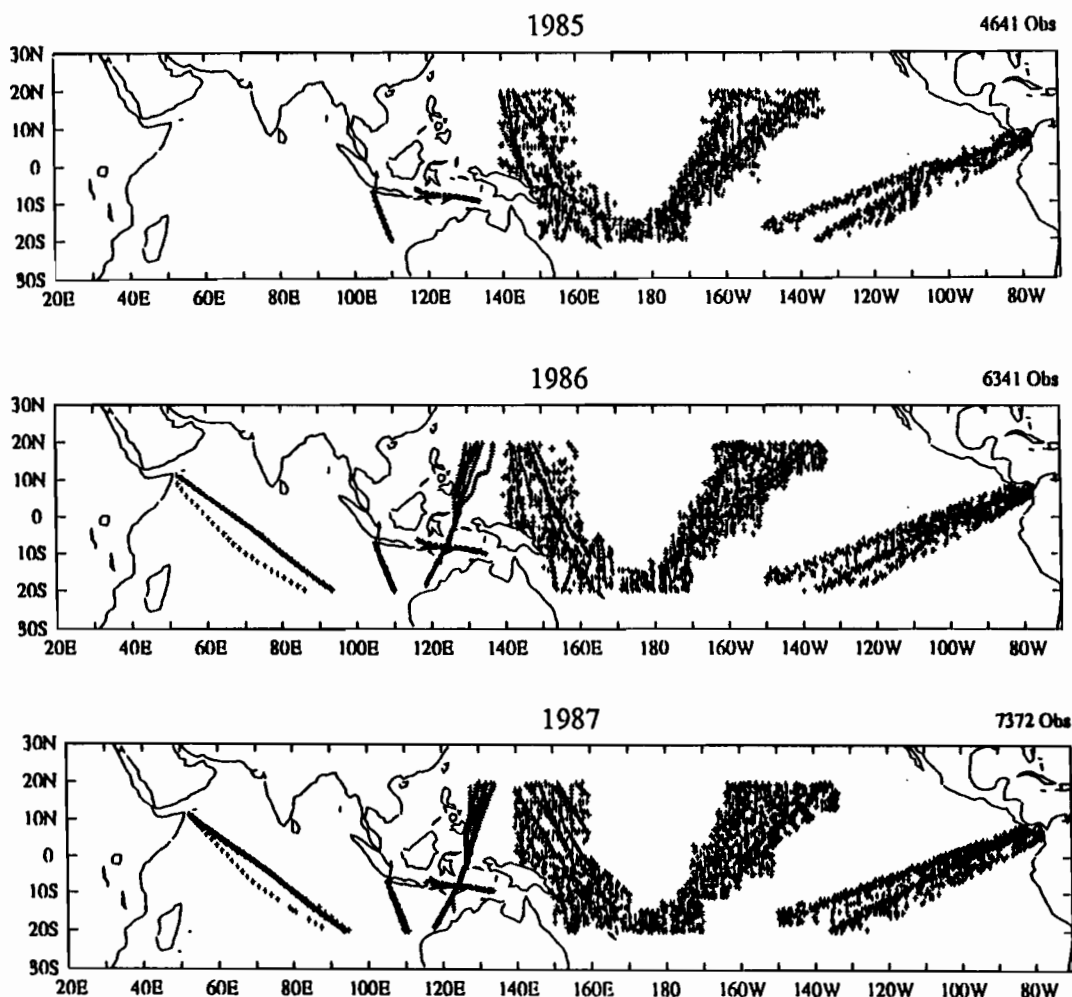


FIG.5. Expendable bathythermograph (XBT) stations used for their study.

The TOGA XBT network (Fig. 5) has provided a data set of high quality temperature soundings in the tropical Pacific and Indian Oceans which can be used to document the near surface thermal structure. For this study we used a subset of the total data set assembled at the TOGA Subsurface Data Center, Brest, France (J.P. Rébert, personal communication), selected to represent the areas where carefully controlled high quality (delayed-mode) data are regularly collected. The data were combined with data from a prototype of the network started in 1979 (Donguy, 1987) and used in earlier studies of the surface heat budget (Meyers et al., 1989a; England et al., 1989).

The mixed layer temperature along the equator in the Pacific was determined near 100°W (Eastern Pacific) 165°W, (Central Pacific) and 160°E (Western Pacific) for the period 1979-1988 to document variability of zonal MLT gradients. The MLT time series are monthly averages, smoothed by a (1/4, 1/2, 1/4) filter, for the latitude band 0°-6°N (Fig. 6) and 0°-6°S (Fig. 7). The 1982/83 ENSO episode stands out as a marked temperature change on both sides of the equator all across the Pacific. The temperature difference between the central and western tracks which usually increases about 1°C toward the west changed sign in July 1982 and rapidly increased to a 1°C anomalous gradient in the other direction. The reversal was preceded by a large (>1°C) increase in central MLT starting in April 1982 and a small decrease in western MLT starting in March 1982 (Fig. 6). The eastern Pacific is usually 2°-5°C cooler than the central Pacific and has a dominant annual oscillation, which reached an ENSO peak in early 1983, when the zonal temperature gradient reversed all the way across the Pacific (Fig. 6).

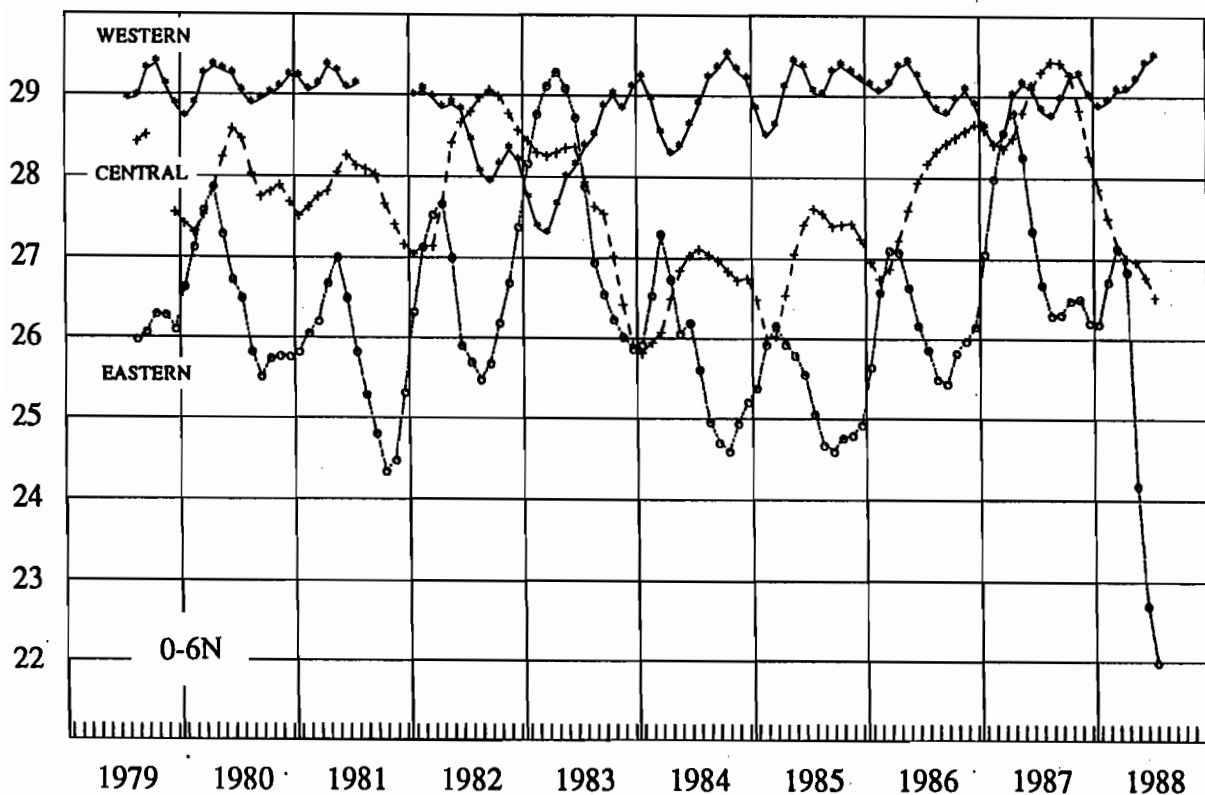


FIG.6. Mixed layer temperature (°C), 0°-6°N, on the western ($\approx 160^\circ\text{W}$), central ($\approx 165^\circ\text{W}$) and eastern ($\approx 100^\circ\text{W}$) XBT tracks

In the 1986/87 ENSO reversal of the MLT gradient between 165°W and 160°E was observed again, primarily south of the equator (Fig. 7), beginning in December 1986. The western MLT dropped rapidly after May 1986, but the temperature at 165°W did not rise enough to make a reversal. Reversal north of the equator (Fig. 6) occurred briefly beginning in June 1987. The weaker intensity of this episode appears markedly in the eastern Pacific temperature. We cannot say on the basis of data in hand whether or not reversal of the MLT gradient along the equator was associated with the onset of 1986/87 ENSO. In the case of a weaker episode the initial reversal may be confined to a small distance along the equator, near the dateline on the eastern edge of the 28°C water pool. The measurements at 165°W may be too far eastward to see it. This highlights the need for more temperature observations in the area between the western and central Pacific XBT line.

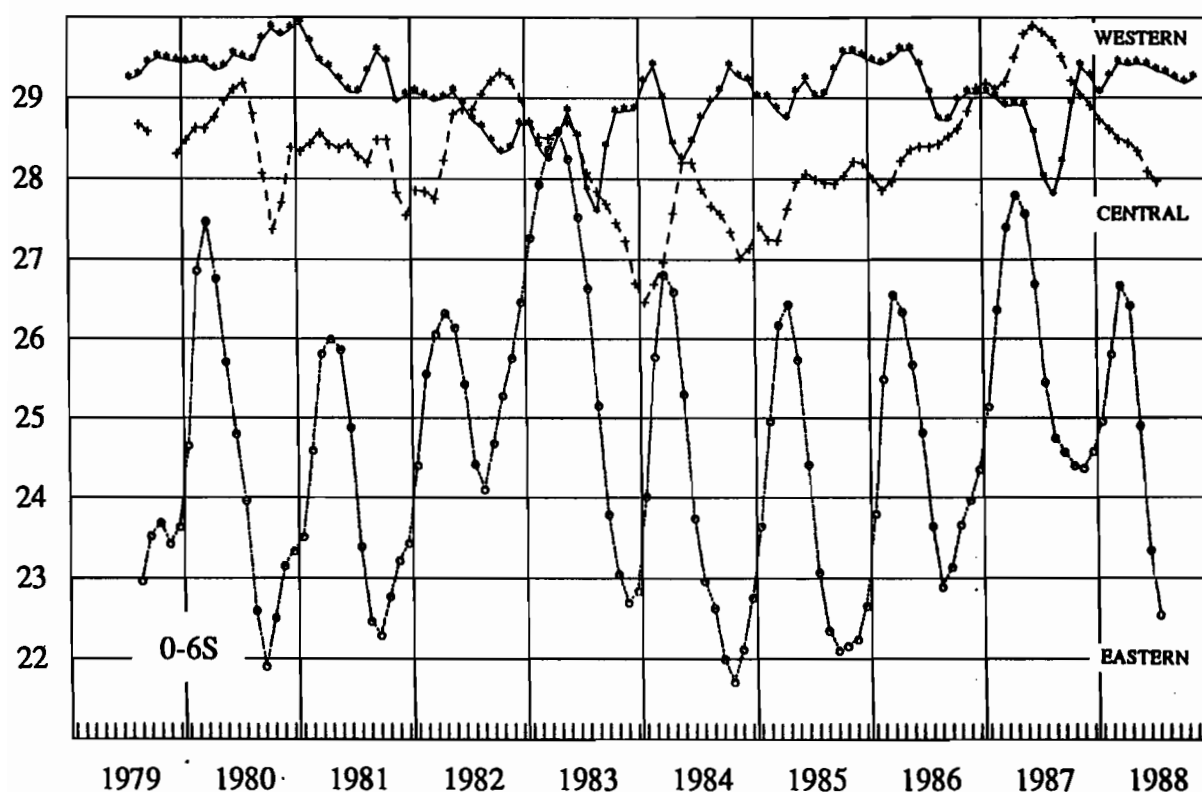


FIG.7. Mixed layer temperature (°C), 0°-6°S, as in figure 6.

Time series of mixed layer depth are presented in figures 8 and 9 in a format that facilitates comparison to MLT. The definition of MLD was the depth at which temperature is 1°C less than SST. It is compared to the result of other definitions of mixed layer depth and to depth of isotherms in the upper part of the thermocline in Meyers et al. (1989a). We have not found any simple direct relationship between MLD and MLT, probably because MLT at any given time is simultaneously influenced by surface fluxes, horizontal advection, and mixing. A data-based parameterization of mixing, in terms of MLD would first require removing the effect of other mechanisms.

MLT and MLD on the tracks west of the three main Pacific tracks suggest that western Pacific cooling during the 1986/87 ENSO extended at least as far westward as the Fremantle-Sunda Strait track (Fig. 10) as did the upward displacement of the thermocline (Fig. 11).

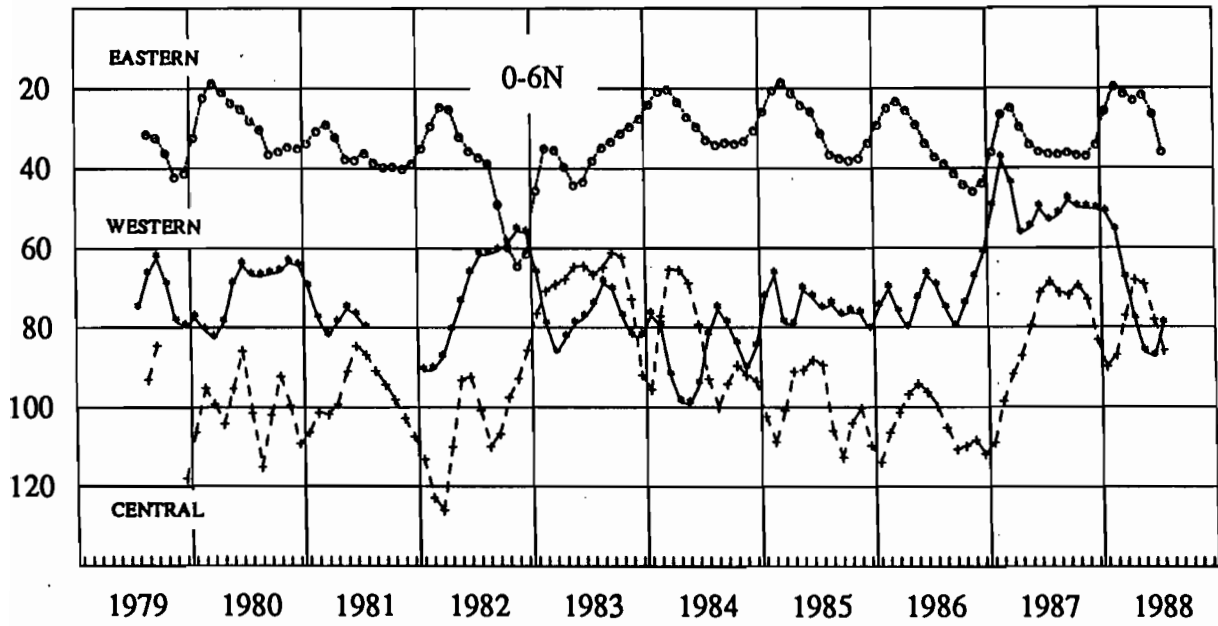


FIG.8. Mixed layer depth (m), as in figure 6.

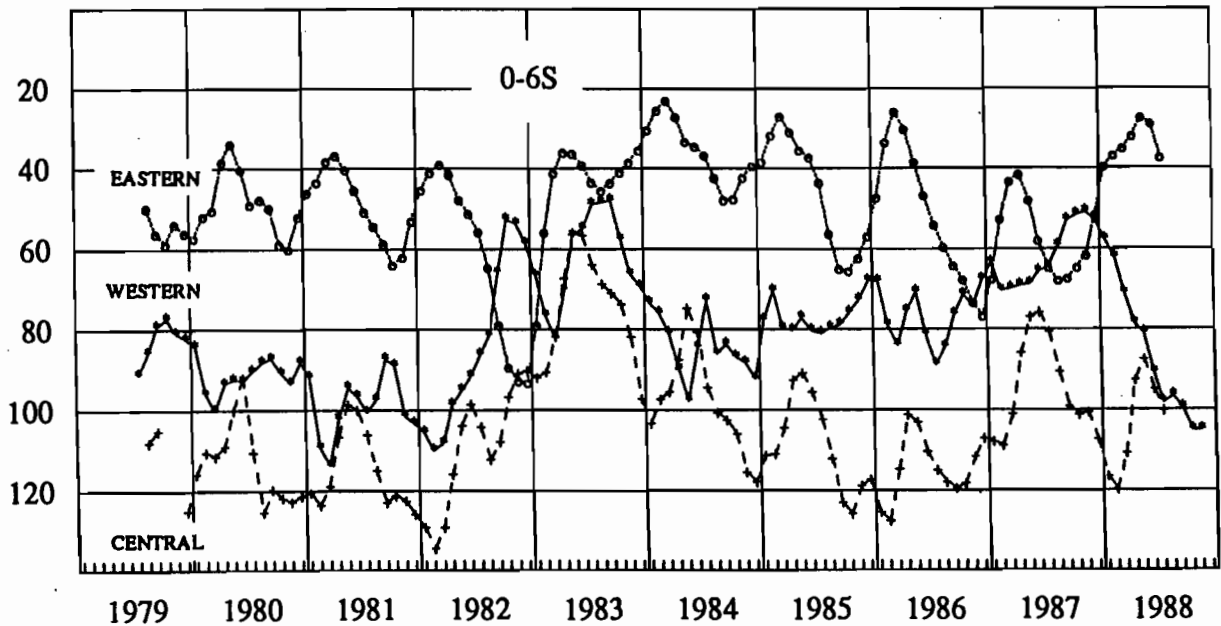


FIG.9. Mixed layer depth (m), as in figure 7.

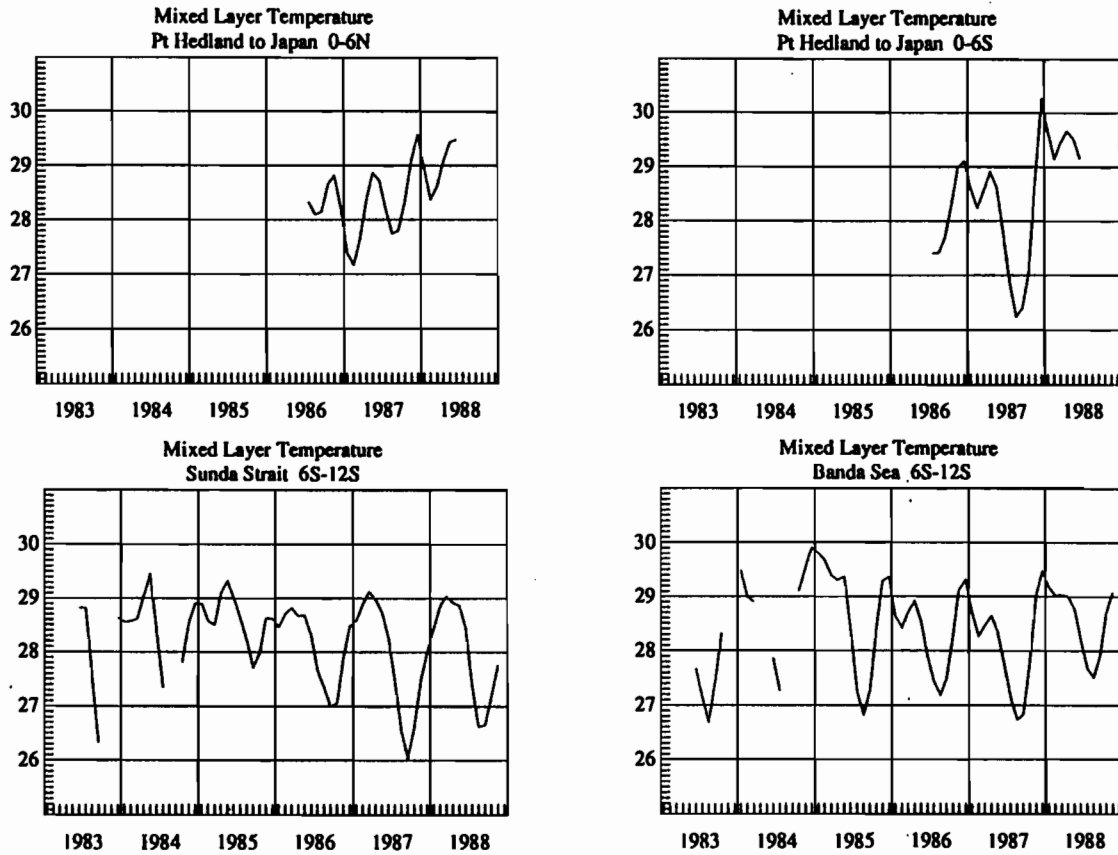


FIG.10. Mixed layer temperature (°C) on XBT tracks in the Indonesian Seas and Indian Ocean.

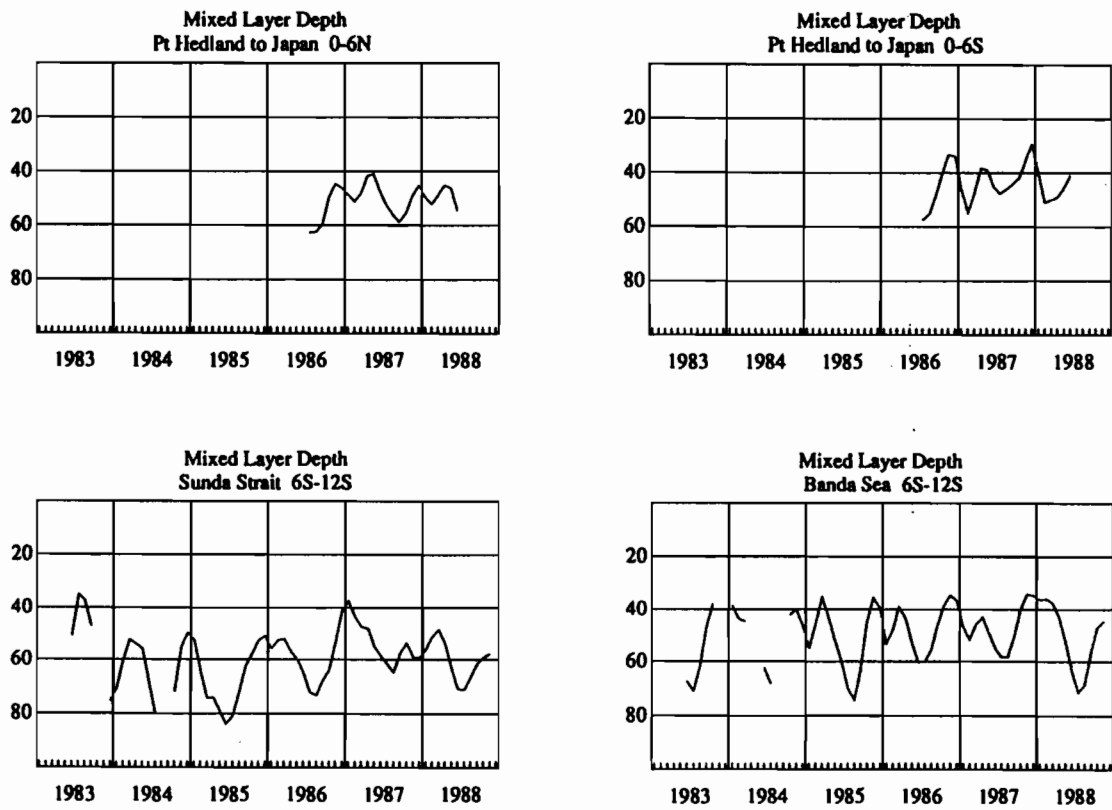


FIG.11. Mixed layer depth (m), as in figure 10.

6. Scales of mixed layer temperature variability

The scales of mixed layer temperature variability were analyzed by empirical orthogonal function (EOF) analysis in order to document differences in spatial scales for the central and western Pacific, and to guide the selection of a grid-size for a study of the surface heat budget. The following is a summary of work discussed in more detail by Meyers et al. (1989a).

The mean and standard deviation of MLT for the period 1979-1984 are presented in Figure 12 for the western, central and eastern tracks. The maximum temperature appears on the western track at 5°S and the central track at 9°S, where temperature exceeds 29°C. Minimum variability occurs at the temperature maximum. Minimum temperature and maximum variability occur in the equatorial cold tongue, on the eastern track near 1°S. The variability represented as standard deviation in Fig. 12 was decomposed into space and time signals using EOF analysis.

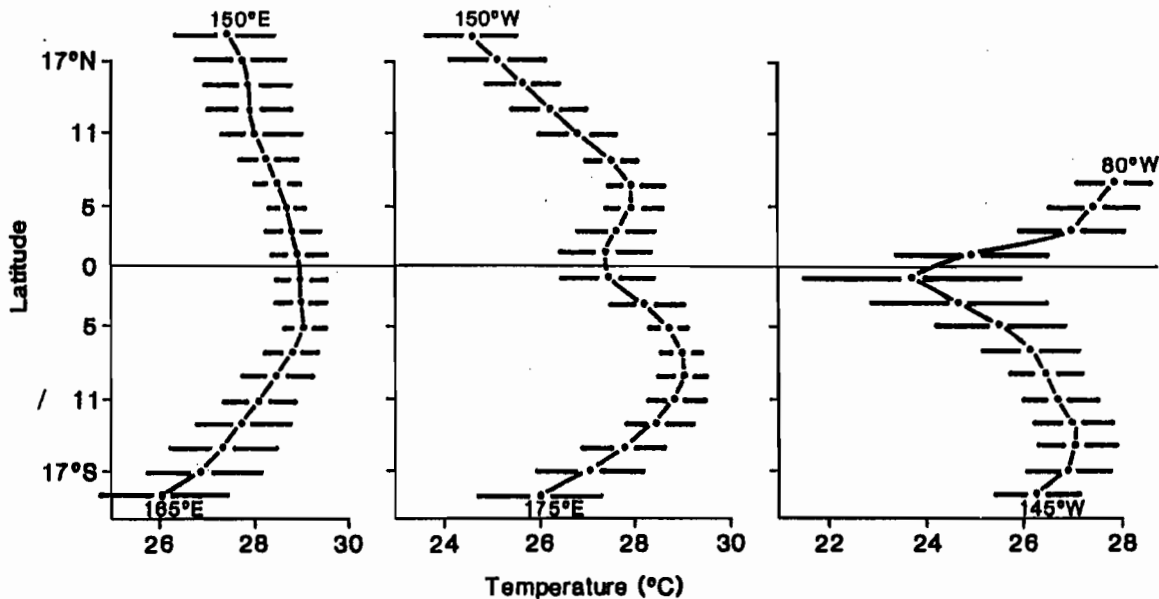


FIG.12. Mean (1979-1984) mixed layer temperature (°C) and ± 1 standard deviation on the western ($\approx 160^\circ\text{E}$), on central ($\approx 165^\circ\text{W}$) and eastern ($\approx 100^\circ\text{W}$) XBT tracks.

The method was applied to time series at each 2° latitude grid point after each series was normalized by standard deviation. The first three spatial (Fig. 13) and temporal (Fig. 14) EOF's represent 76% of the variance. All three EOF's are discussed in some detail by Meyers et al. (1989a). Here we highlight only the second EOF (20% of normalized variance) because the temporal function (Fig. 14) carries the signature of the 1982/83 ENSO. The spatial pattern (Fig. 13) shows a near equatorial signal on the central track confined to 10°N-10°S, indicating warming. A cooling signal appears on the western track in a larger area between 19°N and 19°S. The different spatial scales on the two tracks suggests that different processes may dominate the heat budget in the two regions. It is worth noting that the seasonal oscillation apparent in EOF2 (Fig. 14) during the first three years appears because the central Pacific annual cycle lags the eastern Pacific cycle, by 2-3 months. The annual cycle in the eastern equatorial Pacific and at extra equatorial latitudes was carried in EOF1.

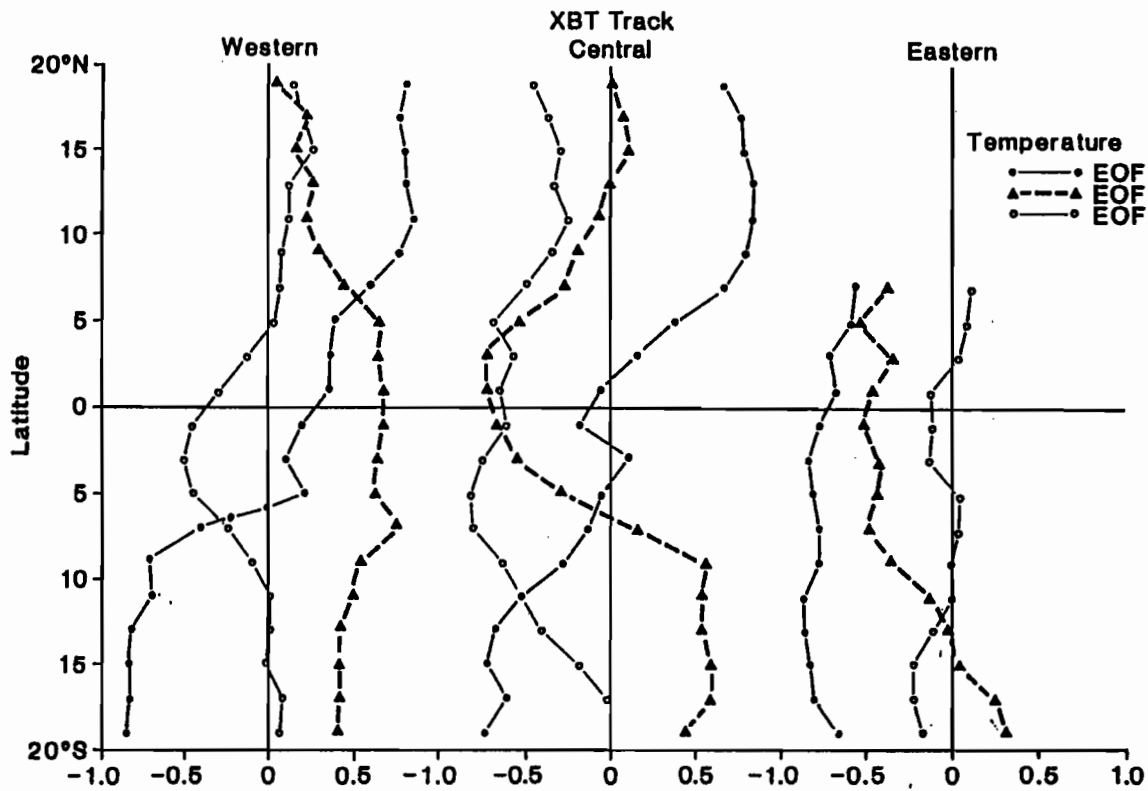


FIG.13. Spatial empirical orthogonal functions of mixed layer temperature.

7. Surface heat budget

The large spatial extent of western Pacific cooling extending from 19°N-19°S and spreading westward through the Indonesian seas into the Indian Ocean suggests an atmospheric origin (Meyers et al., 1986). A study of the influence of air/sea surface heat fluxes on the mixed layer heat budget through out the tropical Pacific is reported here. A study of the complete heat budget including fluxes, advection, mixing and other mechanisms was reported by England and Meyers (1989).

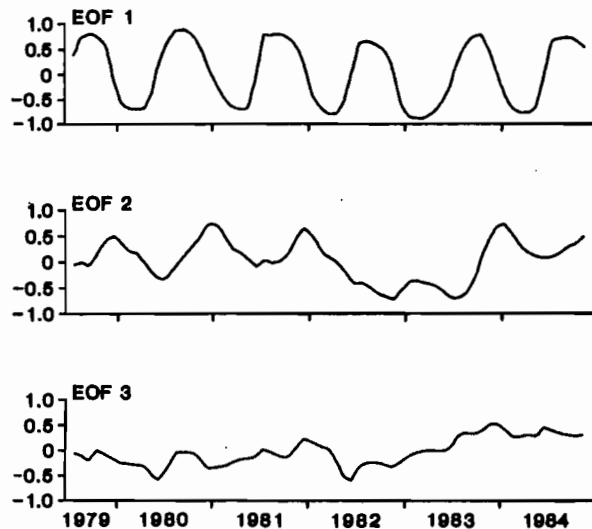


FIG.14. Temporal empirical orthogonal functions for spatial patterns in Fig.13.

	λ	H	σ_H	Q	σ_Q	$r_{H,Q}$	σ_{Q+E}	$r_{H,Q+E}$
12°N-18°N	160°E	-9	66	57	58	.85	62	.86
6°N-12°N	160°E	3	42	47	49	.62	50	.64
0° - 6°N	160°E	2	28	69	30	.49	31	.50
0° - 6°S	160°E	0	28	62	32	.35	33	.45
6°S-12°S	160°E	-5	39	57	54	.51	56	.55
12°S-18°S	160°E	0	60	20	82	.73	82	.75
12°N-18°N	150°W	-2	51	19	37	.69	38	.72
6°N-12°N	160°W	4	34	22	38	.40	38	.43
0° - 6°N	160°W	0	38	67	36	.26	37	.24
0° - 6°S	170°W	-2	51	74	26	.01	28	.04
6°S-12°S	170°W	3	32	54	28	.47	29	.51
12°S-18°S	180°W	0	54	26	65	.72	66	.73
0° - 6°N	100°W	0	31	62	41	.50	41	.52
0° - 6°S	110°W	4	61	125	39	.15	40	.20
6°S-12°S	120°W	-5	57	66	46	.62	47	.64
12°S-18°S	140°W	-7	70	49	45	.77	48	.79

Table 1. Influence of surface fluxes on local heat storage measured in $W.m^{-2}$. Longitude (λ), mean and standard deviation during 1980-1983 of heat storage (H, σ_H), mean and standard deviation of net surface fluxes (Q, σ_Q), correlation between local storage and fluxes ($r_{H,Q}$), standard deviation of net fluxes plus entrainment (σ_{Q+E}), correlation of local storage and fluxes plus entrainment ($r_{H,Q+E}$).

The model of MLT variability tested in this study is a balance between total heat fluxes on the surface (Q) and the local rate of heat storage due to temperature change ($\rho C_p h T_t$) where T_t is the partial derivative of MLT with respect to time, h is MLD, ρ is density, and C_p is heat capacity of water. The model is thus;

$$Q = Q_{sw} - Q_{LW} - Q_s - Q_L \quad ; \quad H = \rho C_p h T_t = Q$$

where H is the local heat storage rate measured by XBT and Q_{sw} , Q_{LW} , Q_s and Q_L are the shortwave, longwave, sensible and latent heat fluxes estimated by the bulk aerodynamic method from weather data.

Before testing the model by correlation analysis, values of Q and H from the 2° latitude grid were averaged over 6° latitude bands on the three main XBT tracks in the Pacific. The

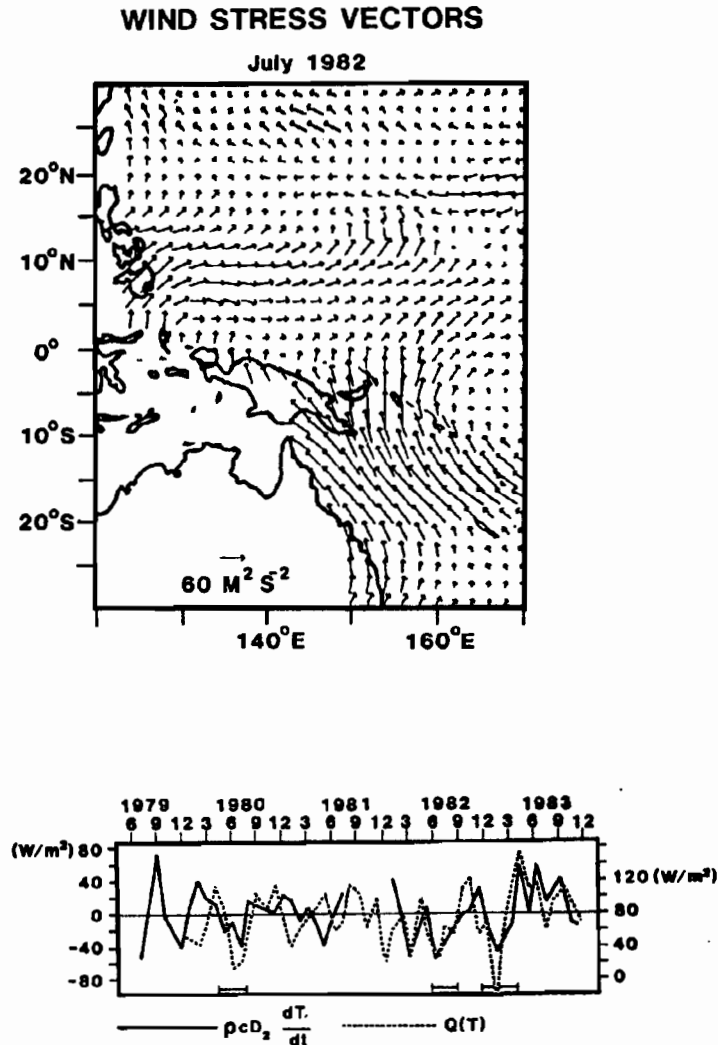


FIG.15. (TOP) Field of wind stress in July 1982. (BOTTOM) Local rate of heat storage measured by XBT (solid line) and total surface heat fluxes ($W \cdot m^{-2}$) estimated by the bulk aerodynamic method using weather data (dashed line).

correlation coefficient (r_{HQ}) are presented in Table 1. (The other statistics in the Table are discussed in Meyers et al., 1989a, and for brevity is not repeated here). The highest values of r_{HQ} occur in the extra equatorial latitude bands because of strong, atmospherically driven seasonal oscillations in temperature. The seasonal oscillation also appears in Q and H in the eastern Pacific 0° - 6° N. Focusing on near equatorial areas where the ENSO signal is most prominent, relatively high correlations extend across the equator in the western Pacific, while they drop to nearly zero in the central and eastern Pacific. The low correlation is consistent with the idea that MLT change during ENSO in the central and eastern Pacific is dominantly driven by anomalous eastward advection and downwelling (Harrison et al., 1989). The higher correlation coefficients in the western Pacific are consistent with the idea that an atmospheric process governs the whole latitude band from 19° N- 19° S. The errors of measurement in Q and H (see Meyers et al., 1989a for estimates) tend to reduce the magnitude of correlation coefficients below that for the values that would be obtained with error-free measurement. Thus the value of r_{HQ} do not indicate how much of the variance of heat storage is accounted for by the model.

A visual comparison of Q and H in the western Pacific (Fig. 15, bottom) helps us understand the cooling process. To a large extent the positive correlation is due to variations during the 1982/83 ENSO. Cooling during ENSO develops when anomalously strong winds blow from subtropical latitudes into the doldrum belt raising the latent heat flux by increasing wind speed (Fig. 15, top). The shortwave and latent heat fluxes throughout the latitude band 19°N - 19°S (Fig. 16) confirm that low values of total flux were associated with peaks of evaporation extending from the subtropics to the equator during the main cooling events, which came from the south during the southern winter and from the north during the northern winter.

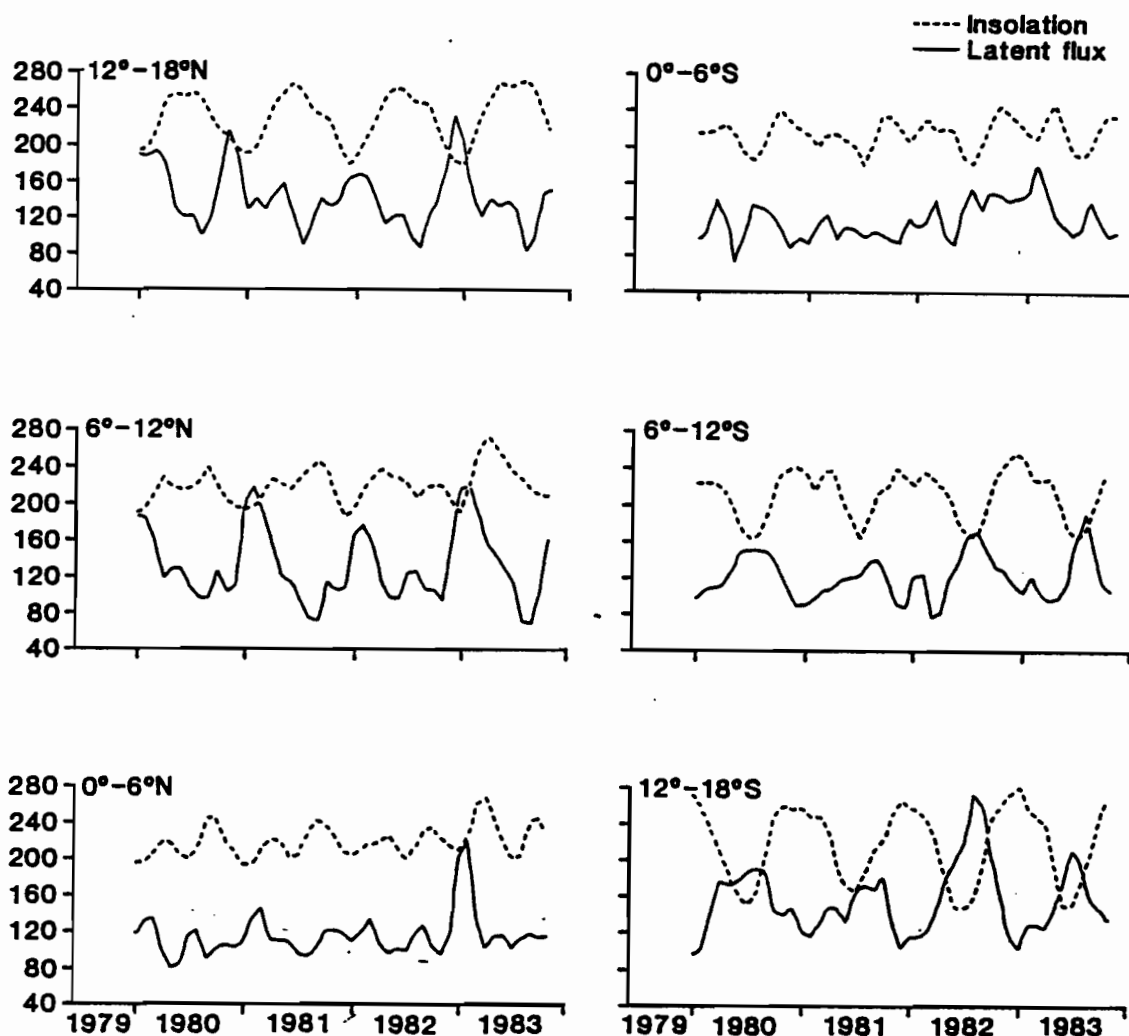


FIG.16. Incoming short wave radiation (W.m^{-2}) and outgoing latent heat flux (W.m^{-2}) near 160°E .

8. Summary and conclusion

The most important results of this study emerged from a study of the heat budget for the 1982/83 ENSO. Firstly a reversal of the temperature difference along the equator between 160°E and 165°W was observed at the onset of the episode, and may indicate that the dy-

namics of a direct thermal cell plays a roll in the onset and growth of ENSO (Lukas, 1988; Meyers et al., 1989a). Secondly, the influence of changes in surface heat fluxes in western Pacific cooling was documented, in contrast to the central Pacific where variability of surface fluxes has little to do with ENSO temperature changes, and anomalous eastward advection and downwelling are thought to be the dominant mechanism of temperature change.

The ENSO episode of 1986/87 had an onset and growth which was similar in some aspects to the 1982/83 episode, however a study of the heat budget for 1986/87 has not yet been completed because currently there is no readily accessible and reliable data base for the heat fluxes between the ocean and the atmosphere (Halpern, 1988).

REFERENCES

- Berlage, H.P., 1966: The Southern Oscillation and World Weather. *K. Ned. Meteorol. Inst., Meded. Verb.*, **88**, 152 pp.
- Cane, M.A., S.E. Zebiak and S.C. Dolan, 1986: Experimental forecasts of El Nino. *Nature*, **321**, 827-832.
- Deser, C. and J.M. Wallace, 1987: El Nino events and their relation to the Southern Oscillation : 1925-1986. *J. Geophys. Res.*, **92**, 14189-14194.
- Donguy, J.R., C. Hénin, A. Morliere and J.P. Rébert, 1982: Thermal changes in the western tropical Pacific in relation to the wind field. *Deep Sea Res.*, 869-882.
- Donguy, J.R., 1987: Recent advances in the knowledge of the climatic variations in the tropical Pacific Ocean. *Prog. Oceanogr.*, **19**, 49-85.
- England, M., and G. Meyers, 1989: The Southern Oscillation and heat storage in the equatorial Pacific Ocean, 1979-1984 : Part II: The influence of ocean dynamics. *J. Mar. Res.*, (submitted).
- Halpern, D., 1987: Observations of annual and El Nino thermal and flow variations at 0°, 110°W and 0°,95°W during 1980-1985. *J. Geophys. Res.*, **92**, 8197-8212.
- Halpern, D., 1988: TOGA and Ocean Processes In : Contribution of Geophysics to Climate Change Studies. Proceedings of IUGG Symposium 15, edited by A. Beiger, R. Dickinsen and J. Kindson, *AGU Monography N° XX, American Geophysical Union*, Washington DC.
- Harrison, D.E., W. Kessler and B. Giese, 1989: Ocean circulation model hindcasts of the 1982-83 El Nino: Thermal variability along the ship-of-opportunity tracks. *J. Phys. Oceanogr.*, **19**, 397-418.
- Hénin, C. and J.R. Donguy, 1980: Heat content changes within the mixed layer of the equatorial Pacific Ocean, *J. Mar. Res.*, **38**, 767-780.
- Lander, M.A. and M.L. Morrissey, 1982: Genesis of twin typhoon associated with a west wind burst in the equatorial Pacific : a case study In: *Proceedings of the US TOGA Western Pacific Air-Sea Interaction Workshop*, USTOGA8, University Corporation for atmospheric Research, Boulder, 163-174.
- Lukas, R., 1988: On the role of western Pacific air-sea interaction in the El Nino/Southern Oscillation Phenomenon In: *Proceedings of the USTOGA Western Pacific Air-Sea Interaction Workshop*, USTOGA8, University Corporation for Atmospheric Research, Boulder, 43-69.
- Lukas, R. and P. Webster, 1988: *Proceedings of the US TOGA Western Pacific Air-Sea interaction Workshop*, USTOGA8, University Corporation for Atmospheric Research, Boulder 207, pp.
- McPhaden, M.J., H.P. Freitag, S.P. Hayes, B.A. Taft and Z. Chen, 1988: The response of the equatorial Pacific Ocean to a westerly wind burst on May 1986. *J. Geophys. Res.*, **93**, 10589-10603.
- Meyers, G., J.R. Donguy and R.K. Reed, 1986: Evaporative cooling of the western equatorial Pacific Ocean by anomalous winds. *Nature*, **323**, 523-526.

- Meyers, G., J.R. Donguy, M. England and R.K. Reed, 1988a: The Southern Oscillation and heat storage in the equatorial Pacific Ocean, 1979-1984. Part 1: Surface heat fluxes and local storage. *J. Mar. Res.*, (accepted).
- Meyers, G., H. Phillips and J. Sprintall, 1989b: Space and time series for optimal interpolation of temperature- Tropical Pacific Ocean. *J. Geophys. Res.*, (submitted).
- Nicholls, N., 1989: Sea surface temperature and Australian Winter rainfall. *J. Clim.*, (in press).
- Pazan, S. and G. Meyers, 1982: Interannual fluctuations of the tropical Pacific wind field and the Southern Oscillation. *Mon. Wea. Rev.*, **110**, 587-600.
- Quinn, W. H., V.T. Neal and S.E. Antunez de Mayolo, 1987: El Nino Occurrences over the past four and a half centuries. *J. Geophys. Res.*, **92**, 14449-14461.
- Rasmusson, E. and T. Carpenter, 1982: Variations in tropical sea surface temperature and surface wind fields associated with the Southern Oscillation El Nino. *Mon. Wea. Rev.*, **110**, 354-384.
- Reed, R.K., 1986: Effects of surface heat flux during the 1972 and 1982 El Nino episodes, *Nature*, **322**, 449-450.
- Trenberth, K.E. and D.J. Shea, 1987: On the evolution of the Southern Oscillation. *Mon. Wea. Rev.*, **115**, 3078-3096.
- Wyrtki, K., 1975: El Nino - The dynamic response of the equatorial Ocean to atmospheric forcing. *J. Phys. Oceanogr.*, **5**, 572-584.
- Wyrtki, K., 1985: Water displacements in the Pacific and genesis of El Nino cycles. *J. Geophys. Res.*, **90**, 7129-7132.
- Wyrtki, K. and G. Meyers, 1976: The trade wind field over the Pacific Ocean. *J. Appl. Meteorol.*, **15**, (7), 698-704.
- Wyrtki, K., B.J. Kilonsky and S. Nakahara, 1988: The IGOSS Sea Level Pilot Project in the Pacific. JIMAR Contribution n° 88-0150 Data Report n° 003, University of Hawaii, 59 pp.

**WESTERN PACIFIC INTERNATIONAL MEETING
AND WORKSHOP ON TOGA COARE**

Nouméa, New Caledonia

May 24-30, 1989

PROCEEDINGS

edited by

Joël Picaut *

Roger Lukas **

Thierry Delcroix *

* ORSTOM, Nouméa, New Caledonia

** JIMAR, University of Hawaii, U.S.A.

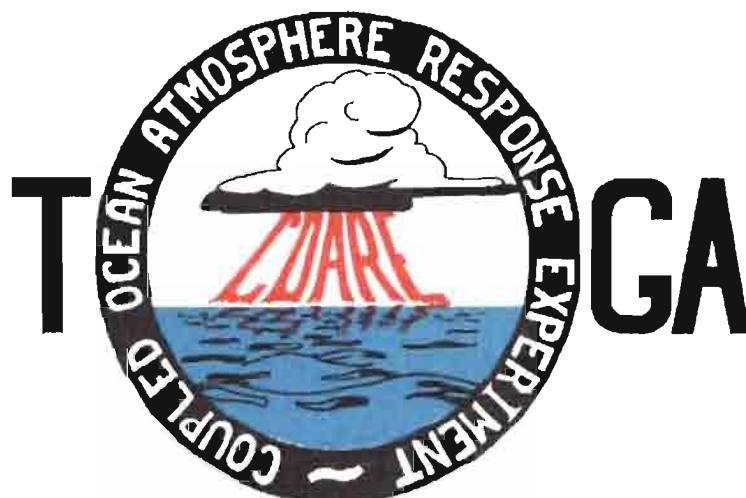


TABLE OF CONTENTS

ABSTRACT	i
RESUME	iii
ACKNOWLEDGMENTS	vi
INTRODUCTION	
1. Motivation	1
2. Structure	2
LIST OF PARTICIPANTS	5
AGENDA	7
WORKSHOP REPORT	
1. Introduction	19
2. Working group discussions, recommendations, and plans	20
a. Air-Sea Fluxes and Boundary Layer Processes	20
b. Regional Scale Atmospheric Circulation and Waves	24
c. Regional Scale Oceanic Circulation and Waves	30
3. Related programs	35
a. NASA Ocean Processes and Satellite Missions	35
b. Tropical Rainfall Measuring Mission	37
c. Typhoon Motion Program	39
d. World Ocean Circulation Experiment	39
4. Presentations on related technology	40
5. National reports	40
6. Meeting of the International Ad Hoc Committee on TOGA COARE	40
APPENDIX: WORKSHOP RELATED PAPERS	
Robert A. Weller and David S. Hosom: Improved Meteorological Measurements from Buoys and Ships for the World Ocean Circulation Experiment	45
Peter H. Hildebrand: Flux Measurement using Aircraft and Radars	57
Walter F. Dabberdt, Hale Cole, K. Gage, W. Ecklund and W.L. Smith: Determination of Boundary-Layer Fluxes with an Integrated Sounding System	81

MEETING COLLECTED PAPERS

WATER MASSES, SEA SURFACE TOPOGRAPHY, AND CIRCULATION

Klaus Wyrtki: Some Thoughts about the West Pacific Warm Pool	99
Jean René Donguy, Gary Meyers, and Eric Lindstrom: Comparison of the Results of two West Pacific Oceanographic Expeditions FOC (1971) and WEPOCS (1985-86)	111
Dunxin Hu, and Maochang Cui: The Western Boundary Current in the Far Western Pacific Ocean	123
Peter Hacker, Eric Firing, Roger Lukas, Philipp L. Richardson, and Curtis A. Collins: Observations of the Low-latitude Western Boundary Circulation in the Pacific during WEPOCS III	135
Stephen P. Murray, John Kindle, Dharma Arief, and Harley Hurlburt: Comparison of Observations and Numerical Model Results in the Indonesian Throughflow Region	145
Christian Henin: Thermohaline Structure Variability along 165°E in the Western Tropical Pacific Ocean (January 1984 - January 1989)	155
David J. Webb, and Brian A. King: Preliminary Results from Charles Darwin Cruise 34A in the Western Equatorial Pacific	165
Warren B. White, Nicholas Graham, and Chang-Kou Tai: Reflection of Annual Rossby Waves at The Maritime Western Boundary of the Tropical Pacific	173
William S. Kessler: Observations of Long Rossby Waves in the Northern Tropical Pacific	185
Eric Firing, and Jiang Songnian: Variable Currents in the Western Pacific Measured During the US/PRC Bilateral Air-Sea Interaction Program and WEPOCS	205
John S. Godfrey, and A. Weaver: Why are there Such Strong Steric Height Gradients off Western Australia ?	215
John M. Toole, R.C. Millard, Z. Wang, and S. Pu: Observations of the Pacific North Equatorial Current Bifurcation at the Philippine Coast	223

EL NINO/SOUTHERN OSCILLATION 1986-87

Gary Meyers, Rick Bailey, Eric Lindstrom, and Helen Phillips: Air/Sea Interaction in the Western Tropical Pacific Ocean during 1982/83 and 1986/87	229
Laury Miller, and Robert Cheney: GEOSAT Observations of Sea Level in the Tropical Pacific and Indian Oceans during the 1986-87 El Nino Event	247
Thierry Delcroix, Gérard Eldin, and Joël Picaut: GEOSAT Sea Level Anomalies in the Western Equatorial Pacific during the 1986-87 El Nino, Elucidated as Equatorial Kelvin and Rossby Waves	259
Gérard Eldin, and Thierry Delcroix: Vertical Thermal Structure Variability along 165°E during the 1986-87 ENSO Event	269
Michael J. McPhaden: On the Relationship between Winds and Upper Ocean Temperature Variability in the Western Equatorial Pacific	283

John S. Godfrey, K. Ridgway, Gary Meyers, and Rick Bailey: Sea Level and Thermal Response to the 1986-87 ENSO Event in the Far Western Pacific	291
Joël Picaut, Bruno Camusat, Thierry Delcroix, Michael J. McPhaden, and Antonio J. Busalacchi: Surface Equatorial Flow Anomalies in the Pacific Ocean during the 1986-87 ENSO using GEOSAT Altimeter Data	301

THEORETICAL AND MODELING STUDIES OF ENSO AND RELATED PROCESSES

Julian P. McCreary, Jr.: An Overview of Coupled Ocean-Atmosphere Models of El Nino and the Southern Oscillation	313
Kensuke Takeuchi: On Warm Rossby Waves and their Relations to ENSO Events	329
Yves du Penhoat, and Mark A. Cane: Effect of Low Latitude Western Boundary Gaps on the Reflection of Equatorial Motions	335
Harley Hurlburt, John Kindle, E. Joseph Metzger, and Alan Wallcraft: Results from a Global Ocean Model in the Western Tropical Pacific	343
John C. Kindle, Harley E. Hurlburt, and E. Joseph Metzger: On the Seasonal and Interannual Variability of the Pacific to Indian Ocean Throughflow	355
Antonio J. Busalacchi, Michael J. McPhaden, Joël Picaut, and Scott Springer: Uncertainties in Tropical Pacific Ocean Simulations: The Seasonal and Interannual Sea Level Response to Three Analyses of the Surface Wind Field	367
Stephen E. Zebiak: Intraseasonal Variability - A Critical Component of ENSO ?	379
Akimasa Sumi: Behavior of Convective Activity over the "Jovian-type" Aqua-Planet Experiments	389
Ka-Ming Lau: Dynamics of Multi-Scale Interactions Relevant to ENSO	397
Pecheng C. Chu and Roland W. Garwood, Jr.: Hydrological Effects on the Air-Ocean Coupled System	407
Sam F. Iacobellis, and Richard C.J. Somerville: A one Dimensional Coupled Air-Sea Model for Diagnostic Studies during TOGA-COARE	419
Allan J. Clarke: On the Reflection and Transmission of Low Frequency Energy at the Irregular Western Pacific Ocean Boundary - a Preliminary Report	423
Roland W. Garwood, Jr., Pecheng C. Chu, Peter Muller, and Niklas Schneider: Equatorial Entrainment Zone : the Diurnal Cycle	435
Peter R. Gent: A New Ocean GCM for Tropical Ocean and ENSO Studies	445
Wasito Hadi, and Nuraini: The Steady State Response of Indonesian Sea to a Steady Wind Field	451
Pedro Ripa: Instability Conditions and Energetics in the Equatorial Pacific	457
Lewis M. Rothstein: Mixed Layer Modelling in the Western Equatorial Pacific Ocean	465
Neville R. Smith: An Oceanic Subsurface Thermal Analysis Scheme with Objective Quality Control	475
Duane E. Stevens, Qi Hu, Graeme Stephens, and David Randall: The hydrological Cycle of the Intraseasonal Oscillation	485
Peter J. Webster, Hai-Ru Chang, and Chidong Zhang: Transmission Characteristics of the Dynamic Response to Episodic Forcing in the Warm Pool Regions of the Tropical Oceans	493

MOMENTUM, HEAT, AND MOISTURE FLUXES BETWEEN ATMOSPHERE AND OCEAN

W. Timothy Liu: An Overview of Bulk Parametrization and Remote Sensing of Latent Heat Flux in the Tropical Ocean	513
E. Frank Bradley, Peter A. Coppin, and John S. Godfrey: Measurements of Heat and Moisture Fluxes from the Western Tropical Pacific Ocean	523
Richard W. Reynolds, and Ants Leetmaa: Evaluation of NMC's Operational Surface Fluxes in the Tropical Pacific	535
Stanley P. Hayes, Michael J. McPhaden, John M. Wallace, and Joël Picaut: The Influence of Sea-Surface Temperature on Surface Wind in the Equatorial Pacific Ocean	543
T.D. Keenan, and Richard E. Carbone: A Preliminary Morphology of Precipitation Systems In Tropical Northern Australia	549
Phillip A. Arkin: Estimation of Large-Scale Oceanic Rainfall for TOGA	561
Catherine Gautier, and Robert Frouin: Surface Radiation Processes in the Tropical Pacific	571
Thierry Delcroix, and Christian Henin: Mechanisms of Subsurface Thermal Structure and Sea Surface Thermo-Haline Variabilities in the South Western Tropical Pacific during 1979-85 - A Preliminary Report	581
Greg. J. Holland, T.D. Keenan, and M.J. Manton: Observations from the Maritime Continent : Darwin, Australia	591
Roger Lukas: Observations of Air-Sea Interactions in the Western Pacific Warm Pool during WEPOCS	599
M. Nunez, and K. Michael: Satellite Derivation of Ocean-Atmosphere Heat Fluxes in a Tropical Environment	611

EMPIRICAL STUDIES OF ENSO AND SHORT-TERM CLIMATE VARIABILITY

Klaus M. Weickmann: Convection and Circulation Anomalies over the Oceanic Warm Pool during 1981-1982	623
Claire Perigaud: Instability Waves in the Tropical Pacific Observed with GEOSAT	637
Ryuichi Kawamura: Intraseasonal and Interannual Modes of Atmosphere-Ocean System Over the Tropical Western Pacific	649
David Gutzler, and Tamara M. Wood: Observed Structure of Convective Anomalies	659
Siri Jodha Khalsa: Remote Sensing of Atmospheric Thermodynamics in the Tropics	665
Bingrong Xu: Some Features of the Western Tropical Pacific: Surface Wind Field and its Influence on the Upper Ocean Thermal Structure	677
Bret A. Mullan: Influence of Southern Oscillation on New Zealand Weather	687
Kenneth S. Gage, Ben Basley, Warner Ecklund, D.A. Carter, and John R. McAfee: Wind Profiler Related Research in the Tropical Pacific	699
John Joseph Bates: Signature of a West Wind Convective Event in SSM/I Data	711
David S. Gutzler: Seasonal and Interannual Variability of the Madden-Julian Oscillation	723
Marie-Hélène Radenac: Fine Structure Variability in the Equatorial Western Pacific Ocean	735
George C. Reid, Kenneth S. Gage, and John R. McAfee: The Climatology of the Western Tropical Pacific: Analysis of the Radiosonde Data Base	741

Chung-Hsiung Sui, and Ka-Ming Lau: Multi-Scale Processes in the Equatorial Western Pacific	747
Stephen E. Zebiak: Diagnostic Studies of Pacific Surface Winds	757

MISCELLANEOUS

Rick J. Bailey, Helene E. Phillips, and Gary Meyers: Relevance to TOGA of Systematic XBT Errors	775
Jean Blanchot, Robert Le Borgne, Aubert Le Bouteiller, and Martine Rodier: ENSO Events and Consequences on Nutrient, Planktonic Biomass, and Production in the Western Tropical Pacific Ocean	785
Yves Dandonneau: Abnormal Bloom of Phytoplankton around 10°N in the Western Pacific during the 1982-83 ENSO	791
Cécile Dupouy: Sea Surface Chlorophyll Concentration in the South Western Tropical Pacific, as seen from NIMBUS Coastal Zone Color Scanner from 1979 to 1984 (New Caledonia and Vanuatu)	803
Michael Szabados, and Darren Wright: Field Evaluation of Real-Time XBT Systems	811
Pierre Rual: For a Better XBT Bathy-Message: Onboard Quality Control, plus a New Data Reduction Method	823